



Methacrylate monolithic stationary phases for gradient elution separations in microfluidic devices

Peter Pruijm^a, Marcus Öhman^b, Peter J. Schoenmakers^a, Wim Th. Kok^{a,*}

^a Analytical Chemistry Group, Van 't Hoff Institute for Molecular Sciences, University of Amsterdam, P.O. Box 94157, 1090 GD, Amsterdam, The Netherlands

^b Department of Chemistry, Karlstad University, SE-651 88, Karlstad, Sweden

ARTICLE INFO

Article history:

Received 2 March 2011

Received in revised form 8 June 2011

Accepted 12 June 2011

Available online 21 June 2011

Keywords:

Methacrylate monoliths

Peptide separations

Gradient elution

Microfluidic devices

ABSTRACT

Methacrylate monolithic stationary phases were produced in fused-silica chips by UV initiation. Poly(butyl methacrylate-co-ethylene dimethacrylate) (BMA) and poly(lauryl methacrylate-co-ethylene dimethacrylate) (LMA) monoliths containing 30, 35 and 40% monomers were evaluated for the separation of peptides under gradient conditions. The peak capacity was used as an objective tool for the evaluation of the separation performance. LMA monoliths of the highest density gave the highest peak capacities (≈ 40) in gradients of 15 min and all LMA monoliths gave higher peak capacities than the BMA monoliths with the same percentage of monomers. Increasing the gradient duration to 30 min did not increase the peak capacity significantly. However, running fast (5 min) gradients provides moderate peak capacities (≈ 20) in a short time. Due to the system dead volume of 1 μL and the low bed volume of the chip, early eluting peptides migrated over a significant part of the column during the dwell time under isocratic conditions. It was shown that this could explain an increased band broadening on the monolithic stationary phase materials used. The effect is stronger with BMA monoliths, which partly explains the inferior performance of this material with respect to peak capacity. The configuration of the connections on the chip appeared to be critical when fast analyses were performed at pressures above 20 bar.

© 2011 Elsevier B.V. All rights reserved.

1. Introduction

Downscaling of liquid chromatography (LC) columns has progressed over the years from capillary LC to Nano LC and recently to the format of microfluidic devices. One of the important driving forces for these developments is the improved efficiency of electrospray ionization (ESI) at lower flow rates because of the smaller amount of liquid that needs to be evaporated [1]. A more efficient ESI process results in more sample ions that can be analyzed by the mass spectrometer, leading to more accurate compound identification and quantification. In the case of proteomics this means that peptides can be identified at lower quantities, resulting in more comprehensive proteome characterization.

Micromachining techniques can be used to manufacture microfluidic devices incorporating injection loops, topographic structured channels, mixers, electrospray nozzles and many more features [2–7]. So, where previously only the chromatographic column was scaled down to a smaller volume, micro technology currently offers the possibility to miniaturize the whole analytical system. The possibility to integrate various components on a single analytical platform gives almost unlimited opportunities for

multiplexing, multidimensional separations and single molecule detection.

From a chromatographic point of view, arrays of pillars in a microfluidic channel may be regarded as an ideal stationary phase [8]. It has been shown that with such channels extremely low plate heights can be obtained in practice [9]. A drawback of the pillar arrays is the low surface area, which makes it difficult to perform interaction chromatography. However, advances are being made towards the production of topographic structures modified with a porous layer to increase the available surface area [10]. Still, there is a long way to go before this approach towards chip-LC will become widespread.

A more straightforward approach for the manufacturing of microfluidic separation devices is by packing a particulate stationary phase in a channel, just as in a conventional column. Various types of stationary phase particles have been packed in microfluidic devices (see e.g. [11], and references therein). Modified silica particles can be packed in channels in polyimide chips that can be used in various modes of chromatography [12,13]. This approach has been made commercially available by Agilent. A convenient alternative for packing of channels with particles is the use of monolithic stationary phase materials in chips. Monoliths can be produced in situ and covalently linked to the channel wall [14–17]. Different polymerization chemistries can be used to produce monolithic materials, but acrylate and methacrylate materials are most

* Corresponding author. Tel.: +31 20 5256539; fax: +31 20 5255604.
E-mail address: W.Th.Kok@uva.nl (W.Th. Kok).

common. Acrylate- and methacrylate-based stationary phases are produced by means of a single-step polymerization reaction which can be initiated thermally or by UV light. The use of UV-initiation would offer an additional advantage: the possibility to precisely determine the position of the retentive phase in the microfluidic device. Moreover, methacrylate monoliths possess a high permeability allowing higher flow rates or low back-pressures, which may be important for devices with pressure limitations.

Methacrylate monolithic stationary phases have been introduced by Svec and Frechet over a decade ago [18] and since that time much effort has been put into the study and development of these materials. This has resulted in a wide range of available materials with different monomers incorporated in the polymer to perform various modes of liquid chromatography [19–25] and in an increased understanding of the factors determining the analytical performance [26–30]. In a fused-silica chip pressure-driven reversed phase separations of peptides and proteins using a stearyl acrylate monolith have been performed in the isocratic mode by Reichmuth et al. [31]. Le Gac et al. [16] performed gradient elution separations of a tryptic digest of Cytochrome C using a lauryl methacrylate stationary phase in a SU-8 based microfluidic device. Levkin et al. have shown separations of peptides and proteins in a chipLC system on different (thermally initiated) organic monolithic stationary phases [17]. In general, however, the performance of systems in chip format is still not matching that of column or capillary formats with packed or monolithic stationary phases [32].

In this paper we describe the production of methacrylate monolithic stationary phases in a channel on a fused-silica chip. The final goal of this study is to explore the possibilities of using such channels as part of a two-dimensional separation system on a chip. For the coupling of two different separation mechanisms the chip format will offer much more possibilities than a column or capillary format. Different reaction mixtures were tested to produce stationary phases that were compared with respect to their chromatographic performance in gradient reversed phase separations of peptide mixtures, and their permeability. Also some practical difficulties were addressed.

2. Experimental

2.1. Materials and reagents

The peptides leutinizing hormone releasing hormone (LHRH, 1), angiotensin 2 (2), [val⁵]-angiotensin 1 (3), substance P (4), renin substrate (5), momany peptide (6), insulin chain B oxidized (7), and melittin (8) were purchased from Sigma–Aldrich (Zwijndrecht, The Netherlands). Numbers between brackets correspond to the numbers used in the chromatograms to identify the peaks. The ingredients of the polymerization mixture, lauryl-methacrylate (99%, LMA), butyl-methacrylate (99%, BMA), ethylene dimethacrylate (98%, EDMA), 1,4-butanediol (99%) and azobisisobutyronitrile (98% AIBN), were also obtained from Sigma–Aldrich. Other chemicals were obtained from standard suppliers and used as received.

2.2. Microchip fabrication

The device consisted of two fused-silica wafers, which were assembled by direct bonding. Before processing, the wafers were cleaned by oxygen plasma and subsequently a wet cleaning with nitric acid. In the bottom wafer the 38 μm deep channel was etched with 25% HF, with a chromium/gold layer as mask material. The 30 nm chromium layer and 120 nm gold layer were deposited by sputter deposition and patterned by photolithography and wet etching. In the top wafer the entrance holes were powder blasted using a Microblaster MB1002 with 29 micron aluminum oxide pow-

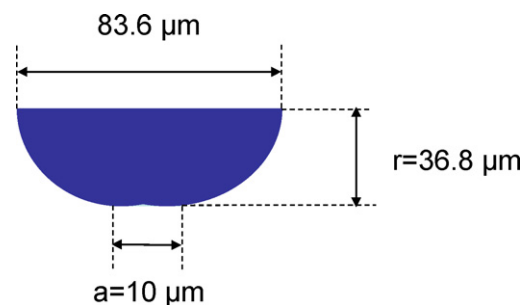


Fig. 1. Schematic representation of the cross section of the channel.

der. The mask material in this case was the photosensitive powder blast foil BF410, patterned by photolithography. After removing the mask material of both wafers and subsequent cleaning, the wafers were aligned and pre-bonded. To fix the bond, the wafer stack was subjected to a temperature treatment at 1100 °C for 1 h and slowly cooled down with a rate of 25 degrees per hour. Finally, the wafer stack was diced into chips with dimensions suitable for the Micronit Lab-on-a-chip kit 4515 (Micronit Microfluidics BV, Enschede, The Netherlands). The channel has a length of 40 mm in a chip of 45 mm \times 15 mm. Fig. 1 shows a schematic representation of the cross section of the channel and its dimensions.

2.3. Preparation of monolithic stationary phases

Poly(butyl methacrylate-co-ethylene dimethacrylate) (BMA) and poly(lauryl methacrylate-co-ethylene dimethacrylate) (LMA) monolithic stationary phases were prepared in fused-silica chips by a single step UV-initiated polymerization reaction. The channel inner wall was vinylized before introduction of the polymerization mixture to ensure anchoring of the stationary phase [33]. The polymerization mixture consisted of BMA or LMA as a bulk monomer and EDMA as crosslinker in a 3:2 (v/v) ratio. Mixtures with 30, 35 and 40% monomers were evaluated. 1-Propanol and 1,4-butanediol were added as porogens in a 4:3 (v/v) ratio. The UV sensitive initiator AIBN was added in amounts of 1% (w/v) with respect to the monomers [34]. The polymerization mixture was sonicated and degassed before use. After injecting the mixture into the microfluidic device, the ends of the connecting capillaries were sealed with pieces of septum. A UV-Crosslinker (Spectroline, Westbury, NY, USA) was used to irradiate the exposed surface for 50 min at 254 nm with an intensity of 3 mW/cm². Before use, the monolith-filled chips were flushed extensively with acetonitrile (ACN) until a stabile back pressure was reached. After that, two fast gradient runs from 0 to 100% ACN were executed in order to remove any remaining porogens and possible particulates that would otherwise have negative effects on the performance of the MS. Then, the chip was wiped clean and interfaced with the MS. A limited number of chips were available and the method of Throckmorton et al. [35] was used therefore to re-use the chips. Chips of which the evaluation was completed, were heated overnight in an oven at 250 °C. After cooling the chips were flushed with a 1 M sodium hydroxide solution to dissolve and remove the – now incinerated – monolith.

2.4. Instrumentation and chromatographic conditions

Reversed phase separations were performed in the gradient mode using an Agilent 1100 series NanoLC system interfaced to an ion-trap mass spectrometer via an Orthogonal Nanospray ion source (Agilent Technologies, Waldbronn, Germany) with a picotip emitter needle of 5 cm length and 8 μm i.d. (New Objective, Woburn, MA, USA). Electrospray ionization was performed at

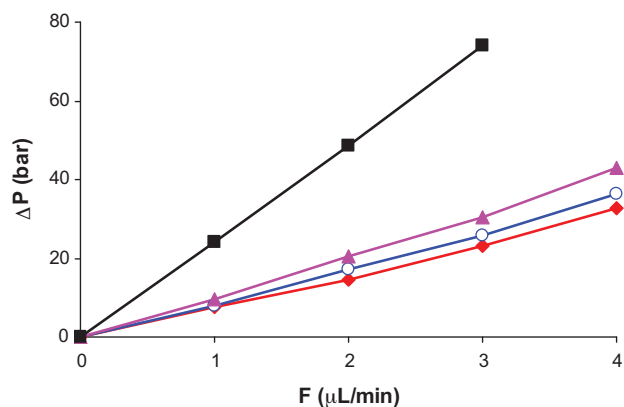


Fig. 2. Plot of back pressure versus flow rate for chips containing 30% BMA (◆), 40% BMA (▲), 30% LMA (○) and 40% LMA (■).

a temperature of 150 °C with a dry-gas flow rate of 6 L/min. The capillary voltage was 1500 V. Data were acquired in the m/z range of 200–2200 at a rate of 20 scans/s.

During all experiments mobile phase A was 0.1% TFA in water, mobile phase B was 0.1% TFA in ACN. All sample concentrations were 10 μg/mL in solvent A and volumes of 50 nL were injected. The microfluidic device was connected to the NanoLC and electrospray emitter needle via a microswitching valve by 25 μm i.d. fused-silica capillaries with a length of 8 cm to minimize external band broadening. Connections to the chip were made using a nut and sealing ferrule and the Micronit Lab-on-a-Chip kit 4515.

3. Results and discussion

3.1. UV-initiated monolithic stationary phases

Methacrylate monoliths were polymerized in the channels using a UV lamp for photoinitiation as described in Section 2. Capillaries were connected to the chip during preparation of the monolith with ferrules that effectively prevented polymerization inside the connection ports. Back-pressures for different monoliths were measured at flow rates up to 4 μL/min of water containing 0.1% TFA. Initially these experiments were difficult to perform because the nanoport connections to the chip started leaking when the back pressure exceeded 20 bar. The nanoport connections consist of a ferrule that closes the entrance hole of the chip and a nut to hold it in to place. Ideally, the ferrule should be partially inserted into the hole in the top layer of the chip so that it touches the entire edge of the hole. Different entrance hole designs were evaluated and the ones with a diameter of 0.6 mm turned out to be the most leak tight. The ferrules needed to be used upside down in order to create stable leak tight connections. The maximum operating pressure of the Micronit Lab-on-a-Chip kit is around 100 bar and in the final set-up this pressure could be maintained without leaking connections. This new configuration also withstands pressure fluctuations better as they occur when a gradient is executed. Fig. 2 shows the back pressures at flow rates of 1–4 μL/min for both BMA and LMA monoliths containing 30 and 40% monomers. The measured back pressures are corrected for the system back pressure. For both the BMA and LMA stationary phases the back pressure is linear with the applied flow rate. There is an increase in back pressure with increasing monomer concentration in the polymerization mixture, and the LMA monoliths show a higher back pressure than the BMA monoliths.

The backpressure characteristics of the monoliths can be quantified with the permeability parameter K , which is defined as [36]:

$$K = \frac{uL\eta}{\Delta P} \quad (1)$$

where u is the superficial mobile phase velocity, L is the length of the channel, η is the solvent viscosity and ΔP is the pressure drop. For the permeability of the 40% LMA monolith a value of $9.8 \times 10^{-14} \text{ m}^2$ was found, for the other monoliths the values were between 2 and $3 \times 10^{-13} \text{ m}^2$. The value for the 40% LMA monolith is close to the results reported by Nischang et al., for capillaries with various diameters and cross-sectional geometries, also obtained with a polymerization mixture containing 40% methacrylate monomers [37]. On the other hand, the permeability for the 40% LMA monolith is similar to what we found earlier for 'low density' (20% BMA) methacrylate monoliths in capillaries, and that of the other monoliths prepared considerably higher [23,28]. Levkin et al. found much lower permeabilities for methacrylate and styrene-based monoliths in microfluidic channels [17]. A possible explanation for the variation in reported permeabilities and for the differences between chip and capillary formats is that the different conditions in the preparation of the monoliths (thermal or UV initiation, a weaker or less homogeneous illumination during photopolymerization) lead to differences in the size of the globules formed. Another possible explanation was brought forward by Nischang et al. in another study [38]. They found that the confinement of monoliths in very narrow capillaries necessitates a fine-tuning of the polymerization conditions; in capillaries with a high surface-to-volume ratio a selective polymerization at the capillary wall may otherwise lead to an excessive permeable monolith in the centre of the capillary. Similar confinement effects had been shown by He et al. [39]. They found that more porous monoliths and a less uniform globule size are produced in capillaries and channels with a diameter approaching that of the globules. As will be shown below, the chromatographic performance of the most permeable monoliths is not satisfactory.

3.2. Peptide separations

A mixture of eight selected peptides was separated on the different stationary phases prepared with different compositions of the polymerization mixture. Gradients were run in 15 min over a range of 0–50% ACN. A flow rate of 1 μL/min was applied. All peptides eluted before the end of the gradient. In Fig. 3A a base peak chromatogram is shown of the separation on the monolith prepared with a reaction mixture containing 40% BMA and EDMA monomers. Late eluting peptides are separated, but some early eluting peptides co-elute. Early eluting peptides give very wide peaks. Better separations were obtained with LMA monoliths. In Fig. 3B and C the separations are shown obtained with a 35% and 40% LMA monolith, respectively. From the LMA monoliths the peptides elute at a higher ACN concentration than from the BMA monolith and retention increases with the monomer content of the polymerization mixture used. The peak shapes are considerably improved with the 40% LMA monolith. This is in accordance with the idea that this monolith has a smaller or more uniform globule size than the other monoliths, as was suggested by its lower permeability.

An important factor in the optimization of reversed-phase separations in the gradient mode is the gradient time or steepness. In general, an improvement of a separation can be obtained by an increase in the gradient time up to a certain limit where the separation performance reaches a maximum value [40]. The effect of an increase of the gradient time to 30 min on the separations obtained on the 40% LMA monolith is shown in Fig. 4A. The chromatogram shows that with a gradient time of 30 min the peaks are seriously broadened, especially those in the first part of the chromatogram.

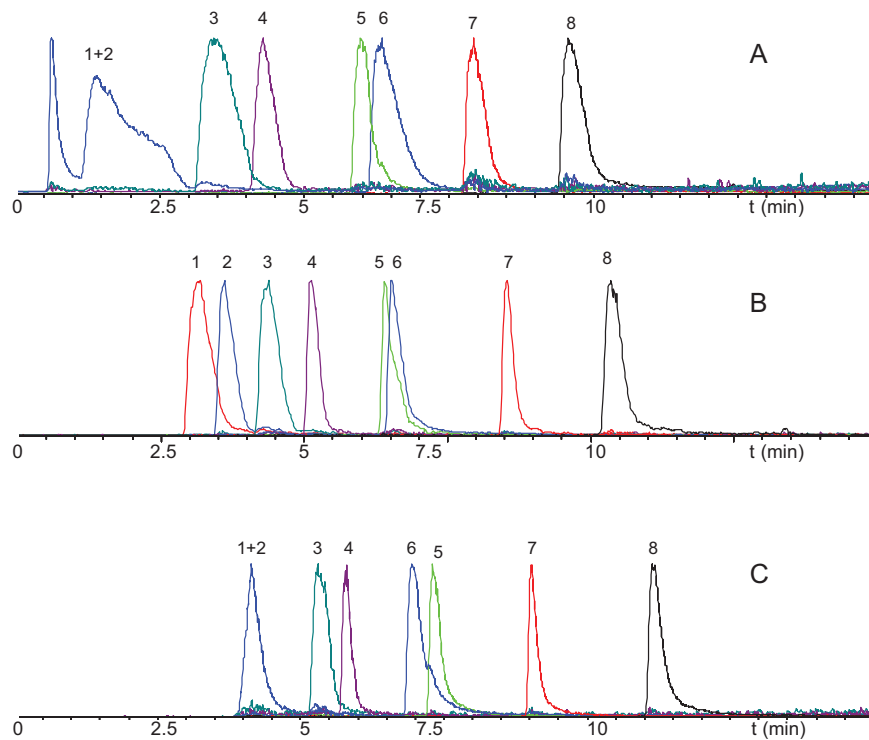


Fig. 3. Effect of the stationary phase composition on the separation of 8 peptides using a channel containing 40% BMA (A), 35% LMA (B) and 40% LMA (C) monoliths with a gradient of 0–50% ACN in 15 min at a flow rate of 1 $\mu\text{L}/\text{min}$. Peaks are labeled with the numbers as in section 2.1.

It should be noted that the gradient at a 15 min gradient time is already very shallow in our experiments. For the gradient steepness the ratio of the column dead time and the gradient time is decisive, and the dead time is short for our monolith filled channels. Making the gradient even more shallow apparently does not help. Similar findings were reported in previous research, where it became clear that the performance of methacrylate monoliths decreases at shallower gradients and so fast and steep gradients are advisable [30].

A possible application of the microfluidic monolith filled channels could be for fast separations as the second dimension in a coupled separation system. Therefore the feasibility of running fast gradients on these chips was also studied. Fig. 4B shows a chromatogram resulting with a gradient run of 5 min on a channel containing 40% LMA, at a flow rate of 1 $\mu\text{L}/\text{min}$. Compared to the

runs with a longer gradient time the time window is smaller, but the peak widths are also strongly decreased.

3.3. Peak broadening

On all monoliths, but especially on the BMA monoliths, early eluting peptides gave wider peaks than late eluting compounds. The difference cannot fully be explained as the result of the injection band width only. An injector with a 50 nL internal loop was used, and this was connected to the channel with a narrow, short piece of capillary with a volume of less than 40 nL. With the expected focusing on the column this is not expected to result in excessively wide injection bands. The strong peak tailing observed may indicate that extra-column band broadening is significant (possibly in the

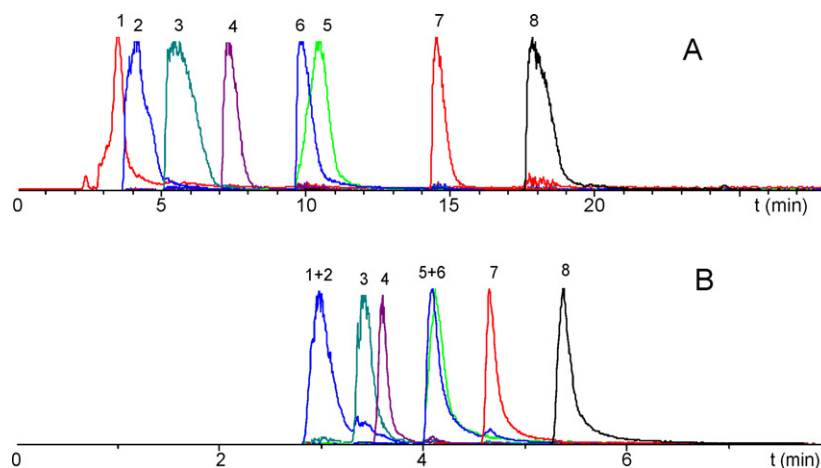


Fig. 4. Effect of the gradient time on the separation of 8 peptides on a 40% LMA monolith using a gradient of 0–50% ACN in 30 min (A) and 5 min (B) at a flow rate of 1 $\mu\text{L}/\text{min}$. Peaks are labeled with the numbers as in Section 2.1.

Table 1
Retention factor in the initial mobile phase and migration distance in the dwell time for chips containing 40% BMA and 40% LMA-EDMA.

Monolith	BMA		LMA	
	k_0	z_D (mm)	k_0	z_D (mm)
Peptide				
LHRH (1)	7.5	40	81	8.1
Substance P (4)	37	17.6	293	2.3
Melittin (8)	784	0.001	3,430,000	0.0002

connection to the mass spectrometer), but this cannot explain that early peaks are wider than late peaks.

Another possible explanation may in be the relatively large dwell volume of the system. The external pump system uses a flow splitter that is physically located at some distance from the injector and the channel. The dwell volume was experimentally determined as 1.0 μ L, while the (mobile phase) volume of the monolith is less than 80 nL. Even though most of the peptides that were separated are large, (relatively) non-polar molecules, the retention factor of some of the model peptides is less than 100 in the initial mobile phase (k_0). In Table 1 the retention factors in the initial mobile phase are given for three of the peptides in the test mixture. The values were either measured directly using the initial mobile phase composition or estimated by extrapolation from measurements with mobile phases with a higher ACN concentration. Low retention factors cause peptide bands to migrate isocratically in the initial mobile phase through a substantial part of the channel. From the retention factors the distance (z) was calculated that the peptides migrate in the channel within the dwell time of the system. The calculations were performed for both the BMA and LMA stationary phase of the highest density. It is clear that all the peptides except for melittin migrate significantly during the dwell time. On the BMA stationary phase the first eluting components will even elute completely under isocratic conditions. For further illustration, the retention factors for the peptides were calculated at every position in the channel for different gradient conditions and stationary phases, using standard theory on gradient elution [41]. As an example, the calculated local retention factors for LHRH, substance P and melittin are plotted against the position in the channel (z) with LMA (Fig. 5A) and BMA (Fig. 5B) monoliths, with a gradient time of 15 min. The effect of the applied gradient is more pronounced for the microchannels containing LMA than for those filled with BMA because it provides more retention and steeper response curves ($\ln k$ versus the volume fraction of organic modifier). From the plots it is apparent that especially on the BMA monolith early eluting compounds migrate with a relatively high average retention factor. In previous research in our laboratory it has been shown that the efficiency of methacrylate stationary phases for peptides and other small molecules strongly decreases with increasing (isocratic and gradient) retention factor [29,30]. Elution at a high retention factor over a part of the column length will therefore give rise to larger contribution to the final plate height. The wide peaks in the beginning of the gradient chromatograms and the low performance of the BMA monoliths in general in our experiments may be explained by this dwell volume effect.

3.4. Chromatographic performance

Peak capacities can be calculated to evaluate the chromatographic performance of gradient systems in a more objective manner. The peak capacity is the number of peaks that can be separated within a certain (gradient) time with a resolution of one. We calculated a conditional peak capacity number that we defined as the ratio of the time window between the first and the last peak for our sample set of 8 peptides and the average peak width at the base of the peaks. The peak capacities as found in our experiments

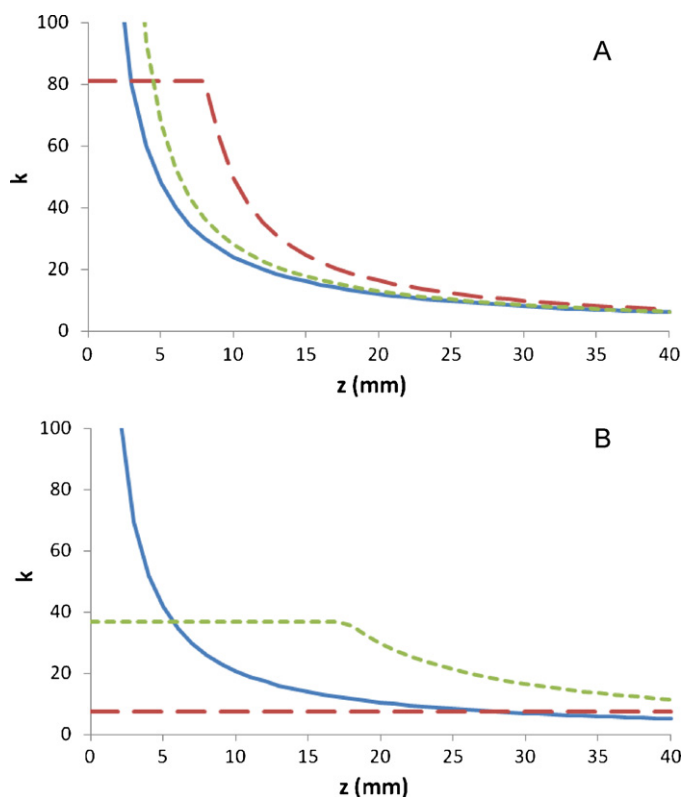


Fig. 5. Plot of the calculated local retention factors (k) for melittin (solid line), substance P (---) and LHRH (...) versus the position in the channel (z) containing 40% LMA (A) and 40% BMA (B) monoliths.

are shown in Table 2. From the table it is clear that when LMA is used as bulk monomer, the peak capacities are higher than for chips containing BMA monoliths. The chips containing 35 and 40% LMA have the highest peak capacities (around 35). The poorest performance is obtained from channels containing 30% BMA monoliths. The effect of the flow rate appeared to be limited. Gradients of 15 and 30 min result in similar peak capacities as could already be seen in the chromatograms in Figs. 3 and 4. Peak capacities were also calculated for fast gradients. The values are lower than those resulting from longer gradients because of the smaller separation window. However, peaks in the steep gradient are more narrow so that the peak capacity is still in the order of 15–20, compared to 20–40 in the 15 min gradients.

The run-to-run and chip-to-chip repeatability was studied for the LMA monoliths. The run-to-run repeatability was assessed from differences in peak retention times and peak widths between duplicate measurements with the same channel, for different monolith compositions, gradient times and flow rates. The variance found between duplicate separations was pooled for all peptide peaks and experimental conditions. Also, the differences in peak capacity between duplicate runs were evaluated. The pooled results,

Table 2
Peak capacities for peptide separations on different monoliths in 5, 15 and 30 min gradients at a flow rate of 1 μ L/min.

Gradient time	Peak capacity		
	5 min	15 min	30 min
30% BMA	12	20	n.d.
35% BMA	13	23	27
40% BMA	18	20	24
30% LMA	10	20	16
35% LMA	16	36	28
40% LMA	22	39	31

Table 3

Run-to-run and chip-to-chip repeatability of gradient separations on LMA monoliths.

Separation parameter	Repeatability (relative standard deviation)	
	Run-to-run	Chip-to-chip
Number of duplicates	8	6
Retention times	1.3%	3.1%
Peak widths	6%	17%
Peak capacities	6%	13%

expressed as relative standard deviations, are given in Table 3. The repeatability of peak retention times (1.3% RSD) is reasonable, although still clearly worse than what is usually found with column or capillary formats [34]. The variation in peak widths and peak capacities between runs is larger. To assess the chip-to-chip repeatability, separations were compared obtained on sets of two different monolith filled channels, with the same type of monolith and under the same experimental conditions (gradient time and flow rate). Again, variances obtained for different sets of channels and experimental conditions were pooled, and the pooled RSD values are included in Table 3. The between-chip variation is clearly larger than the variation between runs on the same chip, especially with respect to peak widths. It should be noted that only chips were included in the repeatability assessment that met certain minimum requirements in terms of performance. Regularly chips were produced with which no separation could be obtained at all. Apparently the production of the monoliths in the channels is still not completely in control.

4. Concluding remarks

This study has shown a number of advantages of methacrylate monolithic stationary phases for chromatography in microfluidic devices. Amongst them, the low back pressure, the simplicity of production and possibility of UV patterning [33] are most important. However, the peak capacities that were obtained in this study with monoliths in a microfluidic channel are insufficient for most real metabolomics or proteomics samples. The short channel length and the relatively large extra column band broadening can be mentioned as explanation for this. A detrimental factor that is specific for methacrylate monoliths is the large dwell volume (compared to the volume of the channel) of the solvent delivery system used in our study. While with other types of stationary phases a large dwell volume will result only in a delay in elution, with methacrylate monoliths it may also cause additional peak broadening. During the dwell time low-retained compounds elute in the isocratic mode, with a relatively high average retention, which is unfavorable for the peak broadening with methacrylate stationary phases. Therefore, the pump system should be adapted in this respect for use with these separation channels. When an external pump with a flow splitter is used, as in our studies, not only the sample injector but also the splitter should be close to the separation channel, in order to limit the dwell volume.

Despite the experimental difficulties and disadvantages mentioned above, there are still some good reasons to opt for methacrylate stationary phases in microfluidic chromatography.

The fast separations that can be obtained with short gradients are attractive when the channel is used for the second-dimension separation in a 2D system. Together with the possibility to create the monolithic bed in a predefined position in a channel system, this offers a large potential for applications in 2D separation systems in a chip format.

Acknowledgements

This research was supported by NanoNed, a nanotechnology program of the Dutch Ministry of Economic affairs (project ASF. 7132). Johan Bomer from the MESA+ institute at the University of Twente is kindly acknowledged for manufacturing the fused-silica chips that were used in this study.

References

- [1] M.S. Wilm, M. Mann, *Int. J. Mass Spectrom. Ion Process.* 136 (1994) 167.
- [2] A. Manz, N. Graber, H.M. Widmer, *Sens. Actuators B* 1 (1990) 244.
- [3] Y. Fintschenko, A. van den Berg, *J. Chromatogr. A* 819 (1998) 3.
- [4] D.R. Reyes, D. Iossifidis, P.-A. Auroux, A. Manz, *Anal. Chem.* 74 (2002) 2623.
- [5] T. Vilkner, D. Janasek, A. Manz, *Anal. Chem.* 76 (2004) 3373.
- [6] P.S. Dittrich, K. Tachikawa, A. Manz, *Anal. Chem.* 78 (2006) 3887.
- [7] M. de Pra, W.Th. Kok, P.J. Schoenmakers, *J. Chromatogr. A* (2007).
- [8] B. He, J. Ji, F.E. Regnier, *J. Chromatogr. A* 853 (1999) 257.
- [9] M. de Pra, W.Th. Kok, J.G.E. Gardeniers, G. Desmet, S. Eeltink, J.W. van Nieuwkaas-teele, P.J. Schoenmakers, *Anal. Chem.* 78 (2006) 6519.
- [10] F. Detobel, S. De Bruyne, J. Vangeloooven, W. De Malsche, T. Aerts, H. Terry, H. Gardeniers, S. Eeltink, G. Desmet, *Anal. Chem.* 82 (2010) 7208.
- [11] K. Faure, *Electrophoresis* 31 (2010) 2499.
- [12] L. Ceriotti, N.F. de Rooij, E. Verpoorte, *Anal. Chem.* 74 (2002) 639.
- [13] H. Yin, K. Killeen, R. Brennen, D. Sobek, M. Werlich, T. van de Goor, *Anal. Chem.* 77 (2005) 527.
- [14] C. Yu, F. Svec, J.M.J. Fréchet, *Electrophoresis* 21 (2000) 120.
- [15] T.B. Stachowiak, T. Rohr, E.F. Hilder, D.S. Peterson, M. Yi, F. Svec, J.M.J. Fréchet, *Electrophoresis* 24 (2003) 3689.
- [16] S. Le Gac, J. Carlier, J.-C. Camart, C. Cren-Olive, C. Rolando, *J. Chromatogr. B* 808 (2004) 3.
- [17] P.A. Levkin, S. Eeltink, T.R. Stratton, R. Brennen, K. Robotti, H. Yin, K. Killeen, F. Svec, J.M.J. Fréchet, *J. Chromatogr. A* 1200 (2008) 55.
- [18] F. Svec, J.M.J. Fréchet, *Anal. Chem.* 64 (1992) 820.
- [19] A. Podgornik, M. Barut, J. Jančar, A. Štrancar, *J. Chromatogr. A* 848 (1999) 51.
- [20] D. Šykora, F. Svec, J.M.J. Fréchet, *J. Chromatogr. A* 852 (1999) 297.
- [21] D. Lee, F. Svec, J.M.J. Fréchet, *J. Chromatogr. A* 1051 (2004) 53.
- [22] Z. Jiang, N.W. Smith, P.D. Ferguson, M.R. Taylor, *Anal. Chem.* 79 (2007) 1243.
- [23] S. Eeltink, E.F. Hilder, L. Geiser, F. Svec, J.M.J. Fréchet, G.P. Rozing, P.J. Schoenmakers, W.Th. Kok, *J. Sep. Sci.* 30 (2007) 407.
- [24] S. Eeltink, L. Geiser, F. Svec, J.M.J. Fréchet, *J. Sep. Sci.* 30 (2007) 2814.
- [25] Z. Jiang, N.W. Smith, P.D. Ferguson, M.R. Taylor, *J. Biochem. Biophys. Methods* 70 (2007) 39.
- [26] E.C. Peters, M. Petro, F. Svec, J.M.J. Fréchet, *Anal. Chem.* 69 (1997) 3646.
- [27] D. Moravcová, P. Jandera, J. Urban, J. Planeta, *J. Sep. Sci.* 26 (2003) 1005.
- [28] S. Eeltink, J.M. Herrero-Martinez, G.P. Rozing, P.J. Schoenmakers, W.Th. Kok, *Anal. Chem.* 77 (2005) 7342.
- [29] Y. Huo, P.J. Schoenmakers, W.Th. Kok, *J. Chromatogr. A* 1175 (2007) 81.
- [30] P. Pruijm, M. Öhman, Y. Huo, P.J. Schoenmakers, W.Th. Kok, *J. Chromatogr. A* 1208 (2008) 109.
- [31] D.S. Reichmuth, T.J. Shepodd, B.J. Kirby, *Anal. Chem.* 77 (2005) 2997.
- [32] K.M. Robotti, H.F. Yin, R. Brennen, L. Trojer, K. Killeen, *J. Sep. Sci.* 32 (2009) 3379.
- [33] C. Yu, M.H. Davey, F. Svec, J.M.J. Fréchet, *Anal. Chem.* 73 (2001) 5088.
- [34] L. Geiser, S. Eeltink, F. Svec, J.M.J. Fréchet, *J. Chromatogr. A* 1140 (2007) 140.
- [35] D.J. Throckmorton, T.J. Shepodd, A.K. Singh, *Anal. Chem.* 74 (2002) 784.
- [36] G. Guiochon, *J. Chromatogr. A* 1168 (2007) 101.
- [37] I. Nischang, F. Svec, J.M.J. Fréchet, *J. Chromatogr. A* 1216 (2009) 2355.
- [38] I. Nischang, F. Svec, J.M.J. Fréchet, *Anal. Chem.* 81 (2009) 7390.
- [39] M. He, Y. Zeng, X.J. Sun, D.J. Harrison, *Electrophoresis* 29 (2008) 2980.
- [40] J.W. Dolan, L.R. Snyder, N.M. Djordjevic, D.W. Hill, T.J. Waeghe, *J. Chromatogr. A* 857 (1999) 1.
- [41] P.J. Schoenmakers, H.A.H. Billiet, R. Tijssen, L. de Galan, *J. Chromatogr.* 149 (1978) 519.